NASA TECHNICAL TRANSLATION NASA TT F-14,698

INVESTIGATION OF COMPACT SOURCES OF COSMIC RADIO RADIATION AT 3.55 cm

D. D. Broderick, L. D. Jauncey, V. L. Efanov, K. I. Kellerman, B. G. Clark, L. P. Kogan, V. I. Kostenko, M. N. Cohen, L. I. Matveenko, I. G. Moiseev.

Translation of "Issledovanie kompaktnykh istochnikov kosmicheskogo radioizlucheniya na volne 3.55 cm" ACADEMY OF SCIENCES. USSR. INSTITUTE FOR SPACE RESEARCH, Report Pr-117, Moscow, 1972, 37 pp.

NATIONAL AERONAUTICS AND SPACE ADMINISTRATION
WASHINGTON, D. C. 20546 JUNE 1973

Abstract

Presented are the results of observations of compact components of quasars and cores of radio-galaxies using a radio-interferometer with an angular resolution limit. The measurements were made at 3.55 cm by the ultra-long interferometry method, with the 22-meter radio-telescope of KAO, Academy of Sciences, USSR, the 42-meter NRAO (USA) and 64-meter NASA (USA) radio-telescopes. The compact components are in most cases complex in structure. Many components have angular dimensions < 0.00025" and linear dimensions < 3 light-months. Their temperature brightness exceeds 10^{12} °K. The temperature brightness of the resolved components lies between 10^{11} - 10^{12} °K.

I

Extraordinarily active and rapidly varying processes occur in a number of cosmic radio sources, such as quasars and the cores of radio galaxies; these processes are accompanied by the emission of galactic energy. This energy is in part converted into the energy of relativistic particles. Relativistic electrons emit light in magnetic fields and create powerful radio radiation, which enables us to "see" these objects. The energies required in order for the radiation to be observed are extremely large. The problem of the origin of this energy and the mechanism by which it is converted into relativistic particles is a basic problem of contemporary astrophysics. Investigation of the physical processes taking place in these objects, and the dynamics of their development, is primarily bound up with a study of their spatial structure. But the sizes of the individual components are extremely small, of the order of one millisecond of arc, and in some instances much less. Measurement of the features of objects with such small dimensions has only recently become possible as a result of the development of the ultra-long interfermeter technique.

These studies were made by American and Soviet radio- /3
astronomers during 1969, at wavelengths of 6 and 2.8 cm [1, 4]. The results of these observations show that quasars and galaxy cores are very complex in structure. In a number of instances the individual components were not resolved, due to insufficiently long baseline or inadequate sensitivity.

Soviet-American interferometric observations of the compact components of quasars and galaxy cores were made on 24-26 July 1971, at 3.55 cm, with the maximum base possible under terrestrial conditions [3].

The measurements were made simultaneously on three radio telescopes: the 22-meter telescope of the Crimean Astrophysical Observatory (KAO, Academy of Sciences, USSR), Simeiz; the 42-meter radiotelescope of the National Radio Astronomical Observatory (NRAO), Green Bank (USA); the 62-meter radio telescope of the Center for Space Communication, NASA, Goldston (USA). On the Simeiz-Goldston base, equal to $270 \times 10^6\lambda$, the limiting angular resolution under terrestrial conditions at 3.55 cm was attained. The width of an interference lobe was 0.00074". The lobe widths on the Simeiz-Green Bank and Green Bank-Goldston bases were respectively, 0.0009" and 0.002". Goldston used a hydrogen frequency standard; rubidium standards were used at Simeiz and Green Bank.

The radio-telescopes were time synchronized prior to the measurements by carrying operating rubidium clocks, and a relative time-check was made from day to day using the Loran-C navigation system signals. The Simeiz and Goldston radio-telescopes used masers; Green Bank used a parametric amplifier.

For the first time all three radio telescopes were equipped with the new Mark II radio-interferometer instrument developed at NRAO (USA). The signals were received in digital form on video tape at a rate of 4×10^6/second. The magnetic tape records were processed at Green Bank on a special computer. /4

The observing program was set up to include sources with compact components at the longer wavelengths [1, 4, 5], with special spectral features at high frequencies and flux components assumed to exceed the computed sensitivity. The sensitivity fluctuation of the radio interferometers with Simeiz-Goldston, Simeiz-Green Bank and Green Bank-Goldston bases were, respectively, 0.1, 0.35 and 0.08 flux units (f.u.).

One basic difficulty in radio interferometric studies is instrument calibration. This difficulty, in the case of a radio interferometer with an angular resolution limit, arises in connection with the lack of calibrating "point" radio sources. Analysis of our observations shows that the radio source OJ 287 can be used as such a source. The amplitude of the interference lobes from this source was the same on all three bases and did not depend on the hour-angle. The interference lobe amplitudes were established with a self-noise system. The radio telescope noise temperatures were measured at various elevation angles and azimuths. The fluxes from other radio sources were determined relative to the flux from OJ 287. In doing this, corrections were made for the changes in noise temperature and effective antenna area with elevation and azimuth angles. The calibration error clearly reduces to the change in the correlated components of the sources examined the same number of times. An estimate of the systematic error shows that it does not exceed 10% (maximum value).

Random errors stem from the following sources:

1. System noise. In this case the r.m.s. error, as noted above, is 0.1, 0.35 and 0.08 flux units for the three different bases. It increases by 20-50% for intense radio /5 sources and low elevation angles.

2. Oscillator instability. The time of coherent storage was selected to be smaller than the maximum permissible averaging time for the rubidium standards used in the experiment [6]; it was ~ 20 seconds. Because of this, the decrease in amplitude of the lobes due to oscillator instability is negligibly small. This effect is even more insignificant in the case of the hydrogen frequency standard.

3. The relative error in establishing the noise temperature of the system. This error is no greater than 3%.

OBSERVATIONAL RESULTS

Results of the observations of the compact components of radio sources are compiled in Table 1. The first column gives the source designation, the magnitude of the total flux F_o in flux units (1 f.u. = 10^{-26} W/m^2 Hz) and the red-shift Z; the second column indicates the base; the third, the time of observation of the source (UT); the fourth and fifth columns give the projections of the base onto the U and V axes, in millions of wavelengths; the sixth column gives the correlated components of the flux F_k in flux units; the seventh column gives the visibility function γ.

The total flux density (daytime observations) was determined from the antenna temperature of the Goldston radio telescope and compared with the results [7]. The 3C 274 was taken as the reference source; its radiation density does not vary with time [7]. The results of the comparison are shown in /6 Fig. 1.

The brightness distributions were calculated on the basis of the observations. Several models were examined for each source, including ellipses with uniform and Gaussian brightness distributions and various sizes and orientations of the axes, two - and three - component models with various flux component density ratios. Graphs of the visibility functions of the models that most nearly fit the experimental points are given for some sources in Fig. 2. In the three curves corresponding to the three bases, the visibility functions are plotted on the ordinates, and the hour-angles of the interferometers, referred to their meridians, are plotted on the abscissa. The geographic projections of the base vectors onto the U-V plane of the source are shown in the upper right corner. The arrows denote the direction of increasing hour-angle. The models are diagrammed at the left side of these figures. For ellipses with a Gaussian distribution, the dimensions are given for a cross section at the level $1/\sqrt{e} \approx 0.62$.

TABLE 1

Source	Base	UT	U	V	F_ν	γ	Remarks
1	2	3	4	5	6	7	8
0j 287	GB-CR	15 06	217	-9	3.4±0.6	0.94±0.16	
F=3.6	GST-CR	17 42	265	29	3.6±0.4	1.0±0.11	
	GST-GB	17 41	59	-17	3.6±0.4	1.0±0.11	
OR 103	GB-GST	23 36	54,3	-6.2	2.8±0,4	0.94±0.13	
F=3,0	GB-CR	23 34	217	13	< 2.4	< 0,8	
	GST-CR	23 33	266	22	2.3±0.3	0,77±0.1	
0K290	GB-GST	17 19	30	-30	2.1±0.3	1.17±0.22	
F=1,8		18 40	58.2	-23.5	1.9±0.3	1.08±0.15	
	GB-CR	16 53	225	5	<2.4	<1.3	
	GST-CR	17 13	253	-15	1.0±0.2	0.56±0.14	
		18 40	265	27	0.8±0.2	0.47±0.15	
0Q208	GB-GST	21 47	36.6	-33.6	2.0±0.3	0.80±0.12	
F=2,5		21 59	40.9	-32.6	2.2±0.4	0.88±0.16	
z=0,077	GB-CR	21 52	22.3	29	< 2.4	< 0.96	
	GST-CR	21 53	252	-4	0.75±0.2	0.30±0.08	
VR0422201	GB-GST	8 14	79.8	-24.2	12.9±1.5	0.96±0.11	
B: LAC		8 30	82.8	-20.4	12.5±1.3	0.93±0.10	
F=13,6		8 42	84.7	-17.4	11.9±1.2	0.89±0.09	
	GB-CR	2 53	185	-75	12.2±1.6	0.90±0.12	
		3 07	193	-68	12.3±1.7	0.91±0.13	
		4 08	215	-34	12.8±1.7	0.95±0.13	
		4 20	218	-26	13.9±1.8	1.09±0.13	
		4 31	221	-19	13.1±1.7	0.97±0.13	
		4 42	223	-12	13.1±1.7	0.97±0.13	
		4 53	224	-5	12,6±1.6	0.93±0.12	
		5 12	225	8	13.0±1.5	0.96±0.12	

1	2	3	4	5	6	7	8
		5 23	225	14	12.5±1.6	0.93±0.12	
		5 37	225	24	11.9±1.5	0.89±0.11	
		5 47	222	31	11.6±1.5	0.86±0.11	
		5 56	222	37	12.3±1.6	0.91±0.12	
		7 03	200	81	8.0±1.4	0.59±0.10	
		7 11	195	86	7.8±1.2	0.56±0.09	
		8 13	161	116	6.7±1.1	0.50±0.08	
		8 25	152	162	7.0±1.2	0.52±0.09	
		8 33	147	125	4.7±0.9	0.35±0.07	
	GST-CR	6 20	265	6	11.9±1.3	0.89±0.10	
		6 25	265	10	12.2±1.3	0.90±0.10	
		6 31	266	15	12.9±1.4	0.96±0.10	
		6 36	266	19	12.3±1.3	0.91±0.10	
		6 41	266	23	11.7±1.3	0.86±0.10	
		6 46	265	27	10.7±1.2	0.79±0.09	
		6 52	265	31	11.4±1.3	0.85±0.10	
		6 57	264	35	11.6±1.3	0.86±0.10	
		7 00	264	37	11.1±1.2	0.82±0.09	
		8 14	240	92	6.1±0.7	0.45±0.05	
		8 19	237	96	7.0±0.8	0.52±0.06	
		8 24	235	100	6.7±0.8	0.50±0.06	
		8 29	232	103	5.6±0.7	0.41±0.05	
NRAO-150	GB-GST	9 44	-8.7	-65.8	5.6±0.7	0.63±0.08	$\gamma = \frac{F_o}{8.9}$
F=10.0		10 43	14.8	-65.2	8.0±0.9	0.90±0.1	
		11 33	34.1	-61.0	7.8±0.8	0.88±0.09	
		12 14	48.6	-55.3	8.9±1.0	1.00±0.1	
		14 06	79.3	-30.4	7.3±0.8	0.82±0.09	*)
		14 29	83.5	-24.1	6.6±0.7	0.74±0.08	
		14 44	85.7	-19.7	6.1±0.7	0.69±0.08	
		14 56	87.3	-16.2	6.1±0.7	0.69±0.08	

*) $\gamma = F_o/8.9$ 11% of the flux equal 1.1 f.u. relative to the resolution on all our base components.

1	2	3	4	5	6	7	8
	GB-CR	9 32	203	-67	< 2.4	< 0.27	
		9 42	209	-57	< 2.4	< 0.27	
		10 43	224	-12	< 2.4	< 0.27	
		11 32	225	25	< 2.4	< 0.27	
		12 15	217	57	< 2.4	< 0.27	
		14 06	208	54	< 2.4	< 0.27	
		14 38	138	147	< 2.4	< 0.27	
	GST-CR	9 44	200	-122	2.2±0.3	0.25±0.03	
		10 44	239	-77	< 0.6	< 0,07	
		11 33	259	-34	1.1±0.2	0.12±0.02	
		12 14	265	2	1.3±0.2	0.15±0.02	
		11 06	243	99	1.5±0.3	0.17±0.03	
		14 41	220	129	1.6±0.3	0.18±0.03	
3C 345 $F = 10.2$ $Z = 0.595$	GB-GST	23 59	27.9	-50	9.2±1	1.03±0.11	$\gamma = \frac{F_o}{9}$
		00 12	32.7	-48.9	8.8±0.9	0.98±0,10	
		00 31	39.7	-46.9	8.6±0.9	0.95±0,10	
		00 44	44.3	-45.5	7,3±0.9	0.87±0,10	*)
		01 15	54.7	-41.1	7.3±0.9	0.81±0.10	
		01 41	62.6	-36.9	7.0±0.8	0.78±0.09	
	GB-CR	21 12	168	-86	3.9±0.8	0.44 ±0.09	
		21 34	183	-74	3.9±0.8	0.44±0.09	
		22 05	199	-57	4.2±0.9	0.46±0.10	
		22 30	209	-43	3.3±0.7	0.36±0.08	
		22 48	215	-32	3.4±0.7	0.38±0,08	
		23 55	225	12	4.2±0.9	0.46±0.10	
		00 06	225	19	4.2±0.9	0.46±0.10	
		00 29	223	33	3.7±0.8	0.41±0.09	
		00 39	221	40	4.1±0.9	0.45±0.10	

*) $\gamma = F_o/9$ 12% flux = 1.2 f.u. relative to the resolution on all our base components.

1	2	3	4	5	6	7	8
		00 17	224	26	4.1±0.9	0.45±0.10	
		00 48	219	45	4.7±0.9	0.52±0.10	
		01 01	216	53	4.2±0.9	0.46±0.10	
		01 11	212	59	4.2±0.9	0.46±0.10	
		01 22	209	66	3.6±0.8	0.44±0.09	
		01 33	204	72	3.7±0.8	0.41±0.09	
		01 44	200	79	4.5±1.0	0.50±0.11	
	GST-CR	23 56	252	-38	3.4±0.5	0.38±0.06	
		00 10	257	-27	3.4±0.5	0.38±0.06	
		01 03	266	11	2.3±0.4	0.25±0.05	
		01 14	266	20	2.3±0.4	0.25±0.05	
		01 24	265	27	2.6±0.5	0.29±0.06	
		01 35	264	35	2.5±0.5	0.27±0.06	
		01 45	263	42	2.6±0.5	0.29±0.06	
4C 39.25	GST-GB	15 50	6.8	-51.7	10.9±1.5	0.99±0.14	
F = 11.2		16 18	18.0	-50.7	9.5±1.5	0.86±0.14	
Z = 0.7		18 10	58.0	-38.8	8.6±1.5	0.78±0.14	
	GB - CR	13 48	163	-88	3.3±0.8	0.3±0.07	
		14 08	176	-78	4.7±0.9	0.43±0.08	
		15 21	212	-38	2.8±0.7	0.25±0.06	
		15 47	220	-21	4.1±0.9	0.37±0.08	
		15 57	222	-14	4.4±0.9	0.40±0.08	
		16 09	224	-8	4.1±0.9	0.37±0.08	
		16 20	225	-1	3.7±0.8	0.34±0.07	
		16 27	225	4	3.8±0.9	0.35±0.08	
		18 09	208	66	3.7±0.8	0.34±0.07	
		18 17	205	71	4.7±0.9	0.43±0.08	
	GST-CR	16 05	236	-60	< 0.8	< 0.07	
		18 09	265	28	1.1±0.2	0.1±0.02	
		19 10	251	72	< 0.8	< 0.07	
3C 84	GST-GB	9 24	-1	-54.8	12.3±1.6	0.29±0.04	
F = 42.5		10 14	18.9	-53.5	15.6±1.9	0.37±0.05	
Z = 0.017		10 59	36.1	-49.9	17.9±2.3	0.42±0.05	
		11 16	42.2	-48	18.8±2.6	0.44±0.06	
		11 20	43.5	-47.5	18.9±2.6	0.44±0.06	
		11 54	55.0	-42.6	18.8±2.6	0.44±0.06	

1	2	3	4	5	6	7	8
		12 33	66.5	-35.8	17.9±2.5	0.42±0.06	
	GB-CR	8 21	197	-62	< 3.0	<0.07	
		9 13	211	-42	3.9±1.0	0.09±0.02	
		9 25	216	-33	5.1±1.1	0.12±0.03	
		09 54	222	-16	3.6±1.0	0.08±0.02	
		10 13	225	-2	3.6±1.0	0.08±0.02	
		11 08	222	35	3	0.07	
		11 52	212	62	3.1±0.9	0.07±0.02	
		12 35	194	86	3	0.07	
	GST-CR	9 24	215	-88	1.7±0.4	0.04±0.01	
		10 12	243	-56	2.5±0.5	0.06±0.01	
		11 05	261	-16	3.2±0.6	0.07±0.01	
		11 17	263	-7	2.6±0.5	0.06±0.01	
		11 53	265	20	2.4±0.5	0.06±0.01	
		12 32	261	50	1.8±0.4	0.04±0.01	
3C 273	GB-GST	20 41	48	4.5	18.9±2.2	0.61±0.07	
F=49		20 49	50.6	4.6	16.1±2	0.52±0.06	
P=0.158		20 56	52.9	4.6	13.6±1.8	0.44±0.06	
	GB-CR	18 41	217	12	4.1±1.0	0.13±0.03	
		19 11	223	13	4.7±1.0	0.15±0,03	
	CR-GST	20 43	265	21	8.6±1.2	0.28±0.04	
		20 54	265	21	8.7±1.2	0.28±0.04	
		20 59	266	22	8.7±1.2	0.28±0.04	
3C 120	GST-GB	13 01	52.8	0.6	4.3±0.6	0.56±0.08	
F=7.6	GB-CR	11 29	225	12	< 2.5	<0.33	
P=0,033	GST-CR	13 01	266	21	1.6±0.4	0.21±0.05	
3C 274	GST-GB	20 22	40.5	-10.6	1.6±0.4		
F=44		21 20	60.0	-7.6	1.8±0.4		
P=0,0041	GB-CR	19 47	224	16	<2.5		
	GST-CR	21 20	262	12	<0.8		

The computations were carried out on the BESM-4 of the Academy of Science's Computing Center. The structures of the compact components of the sources examined, obtained as a result of these computations, are given below.

1. OJ 287. The radio-source OJ 287 has been identified with an optically visible object [8] -- a quasar. Very active processes take place in it that cause rapid changes in the radiation, both optically and in the radio region. In a number of instances the flux from this source fluctuates in the course of several days (Fig. 4) [9, 10], which points to the presence of components of very small angular dimensions. The spectrum of OJ 287 is quite uncertain, but it can be represented about as shown in Fig. 5. By assuming a synchrotron radiation mechanism, the spectrum can be divided into two components A and B (shown dotted). In this case the angular dimensions of the source θ are defined by the following relationship [13]: /13

$$\theta = 1.4 \cdot 10^{-2} F^{1/2} \nu^{-5/4} H^{1/4} (1+z)^{1/4}, \quad (1)$$

where θ is in seconds of arc, F is the maximum flux in flux units, ν is the cut-off frequency (GHz), H is the magnetic field strength in oersteds and Z is the red-shift. The A component has an inflection point at about 1 GHz. The flux density at this frequency is about 1.5 f.u. We shall henceforth assume the magnetic field to be $\sim 10^{-4}$ oersteds. It follows from (1) that the size of the A-component is ~ 0.002". The contribution of radio radiation of this component at 3.55 cm does not exceed 0.4 flux units, as shown in Fig. 5. The B-component is less developed; its spectral inflection point lies in the millimeter-wave range and its maximum flux density is ~ 10 f.u. In this case the angular dimensions of the B-component are no greater than 0.00003". As seen from Fig. 4, the flux density at 2.8 and 4.5 cm increased significantly from the middle of 1970. It can be assumed that at the time of observation the B-component spectrum had been shifted toward lower frequencies (the dash-dot curve in Fig. 5), in which case the angular dimensions, in accordance with (1), should be no greater than 0.00015". The flux density at 3.55 cm at the time of observation amounted to about 3.6 f.u. It is evident from Table 1 that the source OJ 287 has a like correlated flux component on all three bases, i.e. it remains unresolved even on the maximum base ($D_{max} = 270 \times 10^6 \lambda$), and hence its dimensions do not exceed 0.00025". This result corresponds to the size of the B-component. The A-component is resolved, even on the minimum base-line Goldston-Green Bank, regardless of the fact that its radio contribution is small. /14

These results tally with the estimate of the angular size from the source spectrum and define more accurately the results on an adjacent wave [5]. The temperature brightness of the B-component is greater than 2×10^{12} °K.

2. OR 103. This radio-source is apparently a quasar. Its radio flux density is essentially unchanging [7]. It is not resolved on the Green Bank-Goldston base, and the visibility function falls to $\gamma = 0.77$ on the Goldston-Crimea base; from this it follows that its size, assuming a uniform disk, is 0.00034". In this case the brightness temperature is $T_B = 6 \times 10^{11}$ °K. Its size at 3.8 cm is $\theta < 0.0009$" [5].

3. OK 290. This radio-source is obviously a quasar. Its flux density was essentially constant during 1971 [7]. It is not resolved on the Goldston-Green Bank base, and on the Goldston-Crimea base, with $D/\lambda = 254 \times 10^6$ and $D/\lambda = 266 \times 10^6$, $\gamma = 0.56$ and 0.47, corresponding to a circular disk of diameter 0.0005". $T_B = 1.5 \times 10^{11}$ °K. This result is in agreement with the conclusions of reference [5], in which the upper limit of the angular dimension of the source was established as $\theta \leq$ 0.0008" at the nearby wavelength $\lambda = 3.8$ cm.

4. OQ 208. This source, a Seyfert galaxy, has a spectrum with a break at ~ 5 GHz [27]. The flux density at this frequency is 3 f.u. It follows from (1) that the source contains /15 a compact component of size ~ 0.0003". Our experimental results correspond to a circular disk model (diameter 0.0018", $\ell = 2.84$ parsec); its flux is 1.5 f.u. and its core diameter < 0.00025" ($\ell = 0.38$ parsec) with a flux of 1 f.u. This same model is also in accord with the value $\gamma = 0.64$ obtained on the Goldston-Haystack interferometer, with $D/\lambda = 71 \times 10^6$ ($\lambda = 3.8$) [5]. The brightness temperature of the disk is 10^{10} °K and is > 3×10^{11} °K in the core.

5. VRO 42.22.01 (BLLAC). In this object (a compact galaxy), powerful burst processes take place that lead to a rapid fluctuation in the intensity of its radio radiation [7, 14].

The rapid source fluctuation (Fig. 6) [7, 14], and also the increase down to the millimeter-wave spectrum (Fig. 3) [15], is attributable to the high activity and must be associated with the quite complex structure and the existence of compact components of very small angular dimensions.

The experimental data on this source (Fig. 2a) shows a marked change in the visibility function with hour-angle for the Goldston-Crimea and Green Bank-Crimea bases, while the length of the projection of the base on the U-V plane shows practically no change. This circumstance points to an elongation of the source. Experimental values of the visibility function most nearly correspond to a binary-structure with a /16
spacing between components of 0.0005" and an attitude angle of 185°, or, an elliptical disk with a Gaussian brightness distribution, a like orientation and axes of 0.002" x 0.0005".

The increase in the source spectrum down to millimeter waves points to the presence of bright components, whose angular dimensions do not exceed 0.0001". At the same time, a second model to explain the observed flux in the millimeter-wave region on the basis of synchrotron theory (see [1]) requires a magnetic field strength of ~ 10 oersteds, which is scarcely probable. Therefore the most suitable model is one consisting of two point components.

In February, 1971, the distance between components in this source was 0.0009"; its attitude angle was about as before. Thus, in time, the components have drawn together, from 0.0009" to 0.0005". It is difficult to assume that this drawing together actually took place. It is more likely that the "change in distance" is related to the appearance in the course of this time of a third component, or with an intrinsic enhancement of its brightness. In May of 1971 a sharp increase in flux occurred in the centimeter-wave region [7, 14], which could be explained by the formation of a new, bright, compact component.

As seen from Fig. 6, at the instant that this component was observed at 3.55 cm, its flux was about 6.8 f.u. (The flux from this component can be found by assuming it to be equal to the total flux increase of BLLAC relative to the minimum level of 20 April, preceding the burst.) It is natural to assume that its location corresponds to the active core of the galaxy, and the two older components are located symmet- /17
rically with respect to this center, spaced from each other by 0.00085", with a flux of 3.4 f.u. each.

This three-component model, as seen from Fig. 2a, agrees well with the data obtained on all three bases. Since the component dimensions are no greater than 0.0002", $T_B \geq 2.5 \times 10^{13}$ °K in the central component and $T_B \geq 1.25 \times 10^{12}$ °K in the extreme components.

6. NRAO-150. This source does not coincide with any optical object. It has a rather complex spectrum (Fig. 3) in which three components can be distinguished [19]. In 1971 the radio flux density from this source in the centimeter-wave region did not exhibit any rapid fluctuations; only a slow rise was observed [7].

The angular dimensions of its components, as calculated from the spectrum (1), are θ_B = 0.012", θ_C = 0.0003". At 3.55 cm, component C was predominant. The experimental findings are shown in Fig. 2b. The hour-angle dependence of the visibility function on the Goldston-Green Bank and Goldston-Crimea bases indicates that the source has an elongated structure, and the presence of a dip in the visibility function on the Goldston-Crimea base at the instant t = -2.4h indicates that the source is either double or its structure is such that the brightness falls off rapidly toward its edges -- for example, a uniform elliptical disk. Feg. 2b shows curves of the visibility function for an elliptical disk with uniform brightness, comprising 89% (8.9 f.u.) of the flux of the entire source, with axes of 0.0014" x 0.0005" and an attitude angle of 60°. The brightness temperature is 3×10^{11} °K. The remaining 11% (1.1 f.u.) of the flux is radiated by the A and B components, which are completely resolved on our bases. Interferometric /18 tracking of this source at 1665 MHz [4] a size of 0.0013" was found for the C component, which agrees well with our results.

7. 3C345. The source 3C345 is a quasar with a complex spectrum (Fig. 3) [15]. The component sizes, according to this spectrum, should be θ_A = 0.14", θ_B = 0.005", θ_C = 0.0001". About the same sizes for the A and B components were found in interferometric studies at 5000 MHz, 1665 MHz [16] and 400 MHz [17, 18].

The rather high component correlation on the Goldston-Crimea and Green Bank-Crimea bases and its considerable variation on the shortest base (Goldston-Green Bank) points to a source having two components of much different sizes. An analysis has shown that the best agreement with the experimental findings is obtained with a model consisting of an elliptical disk with a Gaussian distribution and axes of 0.0009" x 0.0002" (10.7 x 2.4 persec) and a core diameter of 0.0002" (2.4 persec). The major axis of the ellipse lies along the U-axis (attitude angle 90°) (Fig. 2c). Both components

have about the same flux (4.5 f.u.); T_B = 2.5 x 10^{11} °K and 1.5 x 10^{12} °K for the larger and smaller components, respectively. The remaining 12% (1.2 f.u.) of the flux relates to the components resolved on all three bases, i.e. size > 0.004 (components A and B).

The interferometer studies of this source at approximately the same wavelength (λ = 3.8 cm) [5] have shown that it can be represented by two models: (1) a two-point model with a component spacing of 0.00086" and, (2) an elliptical disk with axes of 0.00095" and 0.00045". The attitude angle for both models is 103°. The visibility function for the two-point model should have been minimum on the GreenBank-Crimea and Goldston-Crimea bases, which was not observed. The second model agrees better with our experimental findings. /19

8. 4C39.25. The radiation flux density of this source grows steadily in the centimeter region; only smooth changes in flux with time are observed [7].

The spectrum of this quasar contains an inflection (Fig. 3) at a frequency ~ 10 GHz; this corresponds to an angular size of ~ 0.0003". A disk model, with a Gaussian distribution of brightness, diameter 0.0004" (5.6 parsec) agrees quite well with the experimental findings (Fig. 2d). $T_B \simeq 1.6 \times 10^{12}$ °K. A brightness function γ = 0.79 was found in reference [5] for a base of 85 x $10^6\lambda$ (λ = 3.8 cm); this agrees well with the experimental data. At a wavelength of 6 cm [4] this component has a size $\leq$ 0.0004".

9. 3C84. The flux density from this source (a Seyfert galaxy) is constantly increasing, and at the end of 1970 an increase in the rate was noted [7]. This attests to the constant activity of the processes in the galaxy's core. The angular dimensions of the compact components should here be very small. The source spectrum is complex (Fig. 3) and consists of three principal elements [19], corresponding to individual spatial components. Components A and B have dimensions of 5' and 0.02" [16] and are completely resolved on all three bases. In this case the observations relate to the C component, which [16] is assigned a disk shape of diameter 0.0025". A model consisting of an elliptical disk with a Gaussian distribution of brightness, containing 94% (40 f.u.) of the flux, with axial dimensions of 0.0021" x 0.0011" (0.72 x 0.38 parsec) and an attitude angle of 17° and a component unresolved on all of our bases (θ < 0.00025", (3.2 light months)) /20

containing 6% (2.5 parsec) of the total flux (Fig. 2e), gave best agreement with the experimental findings. The brightness temperatures of the elongated component and the core are 2.5×10^{11} °K and 7×10^{11} °K, respectively.

10. 3C273. This quasar has a variable flux density in millimeter and centimeter regions [2, 7, 12]. The variation in flux density in the 3-cm region in a number of instances takes place over several months, which corresponds to an unusually small angular size of a component, of the order of 0.00005". During the observing period no substantial activity changes were observed. The spectrum of the source is complex, consisting of several components (Fig. 3) [19]. The size of the high-frequency component D, in accordance with (1), is ~ 0.0001". This dimension pertains to some average active region, whose individual components may be much smaller in size and correspond to the above estimate. The C-component has an angular size of ~ 0.0015".

Interferometer trials at longer wavelengths show that the B, C and D components have sizes of 0.022", 0.002" and < 0.0004", respectively [4]. /21

The results in this paper are in good agreement with a disk model, size 0.0025" (7.9 parsec) and a flux of 22 f.u. and two compact components (< 0.00025") located within the disk and spaced by 0.0015" (4.7 parsec). The radio flux density of each of these components is 4.4 f.u. The disk dimensions agree well with the size of the C-component, as given above. The two-point structure obviously relates to the D-component. The brightness temperature of the disk and core are $T_B = 8 \times 10^{10}$ °K and 1.5×10^{12} °K, respectively. The B-component is much larger in size and is resolved on all three bases.

11. 3C120. In this Seyfert galaxy occasional very strong bursts occur that result in sharp flux density changes. In particular, a flux increase occurred at mid-year of 1970, after which the flux remained constant [7]. The spectrum of this object is complex, consisting of several components, including some in the millimeter and centimeter regions (Fig. 3). In this source, Feb.-Nov. 1971, component scattering with a velocity greater than the velocity of light (v/c = 2 [20]) was observed. As in reference [20], two models were considered: a circle and a binary structure. For comparison, Table 2 shows the models of the compact component obtained at a different time.

The linear velocity of dispersion of the v-components was related to the distance to the source D, its red shift Z and the observed angular velocity $\Delta\theta/\Delta t$ as follows [21, 22]:

$$v = \frac{c}{H} \frac{\Delta\theta}{\Delta t} z. \quad (2)$$

where H = 75 km/sec·Mps is the Hubble constant.

If we substitute into (2) the data from Table 2 on the dispersion of the components in the binary structure, we find that v = 1.6C and 2.1C for the time periods of February-June and June-November, respectively. The rate of increase in sizes of the components from (2), according to Table 2, is > 1.2 and 3.1C for the same time periods. The fact of exceeding the observed dispersion velocity of the components in some sources has been discussed in references [5, 20].

The findings of this work corroborate the conclusions of reference [20] that the rate of expansion of the components exceeds their dispersion velocity. In addition it should be noted that from February-November 1971 there was an acceleration of the dispersion and expansion of components in the 3C120 source.

Table 2

TIME		28.II.71 [20]	25.VI.71 this paper	3.XI.71 [20]
Circle	Diameter (seconds of arc)	0.0014	0.0018	0.0025
Binary Structure	Distance between components, sec. of arc.	0.001	0.0013	0.0017
	Size of component (seconds of arc)	<0.0005	0.0007	0.0013
	Attitude angle (deg.)	95	85	85

/23

12. 3C274. The radio-source 3C274 is the huge elliptical galaxy M87, containing a compact core and a discharge of matter in the form of an elongated blob. The spectrum of the radio-source decreases in the range 10-5000 MHz and contains no details; the spectral index $\alpha = 0.81$ [23]. It is possible that the spectrum of the core is more complex, but its relative contribution to the radio radiation is small, and hence it does not change the overall spectrum of the source. This latter may be the reason for the lack of any marked variation in the flux in the centimetric range [7]. Radio-interferometer studies of the compact component at 13 and 3.8 cm [5, 24, 25, 26] have revealed that the core contains a component with a diameter 0.01" and a smaller component of diameter 0.001". The flux density of the radio radiation of the small component increases with decreasing wavelength, from 1 f.u. to 2 f.u. at wavelengths of 13 and 3.8 cm, respectively.

If this rise in the spectrum of the compact component is determined by reabsorption, the maximum should occur at ~ 5 GHz, with a corresponding flux maximum of ~ 2 f.u. In this event we get from (1) that the size of the compact component should be 0.0003". The flux correlation was 1.7 f.u. on the Green Bank-Goldston base, and the components were completely resolved on the other two bases. Hence the compact component, which possesses the entire flux of 1.7 f.u., has a size of 0.001" (3.1 light months). This deduction agrees satisfactorily with reference [5]. Some dispersion between this value and the size as found from the spectrum of the compact component may be explained by a magnetic field in the source larger than 10^{-4} /24 oersteds.

13. 3C144. In the central region of the Crab nebula is a compact source - a pulsar. Interference lobes were not observed on a single one of the bases, from which it follows that its flux is less than 0.8 f.u. or that the size of the compact source is larger than 0.003".

CONCLUSION

The findings point to the presence of compact components in a number of radio-sources; their angular dimensions are < 0.00025", i.e. less than the angular resolution attainable at 3.55 cm on the maximum base-length possible on earth. A further increase in angular resolution is possible only by decreasing the wavelength or by carrying one of the interferometer elements into space. An increase in angular resolution is of major importance in studying the nature of the radiation from the compact components.

As the observations show, the brightness temperatures of components with angular sizes > 0.001" amounts to 10^{11} - 10^{12} °K. This radiation can be explained within the context of the synchrotron mechanism. But the more compact components have brightness temperatures above 10^{12} °K, and the interpretation of their nature encounters certain difficulties [19]. In this connection the dynamics of the components in their initial stage of development is especially interesting. Here it is necessary to make regular observations, on bases of maximum and intermediate lengths, over a wide range of wavelengths in the centimeter band. This permits studying the spectra of the components, their sizes, spacing and their temporal variations. /25

REFERENCES

1. Broderick, D. D. et al. Astron. zh., 47, 1970, 784.
2. Kellermann, K. I. and Pauling-Toth, I. K. K. Ann. Rev. of Astron. and Astrophys., 6, 1968, 417.
3. Clark, B. G. et al. Astron. zh., 49, 1972, 700
4. Kellermann, K. J. et al. Astrophys. J., 169, 1971, 1.
5. Cohen, M. H. et al. Astrophys. J., 170, 1971, 207.
6. Kogan, L. R. Izv. VUZ, Radiofiz., in press.
7. Medd, W. J., Andrew, B. H., Harvey, G. A. and Locke, J. L. Preprint, Astrophys. Branch, NRCC, 1972.
8. Blake, G. M. Astroph. Letters, 6, 1970, 201.
9. Kinman, T. D. and Condin, E. K., Astrophys. Letters, 9, 1971, 147.
10. Andrew, B. H., Harvey, G. A. and Medd, W. J. Astrophys. Letters, 9, 1971, 151.
11. Gorshkov, A. G. et al. Astron. tsirkulyar 545, 1970.
12. Fogarty, W. G., Epstein, E. E., Montgomery, J. W. and Dworetsky, M. M. Astron. J., 76, 1971, 537.
13. Slysh, V. I. Nature, 199, 1963, 682.
14. Macleod, J. M., Andrew, B. H., Medd, W. J. and Olsen, E. T. Astrophys. Letters, 9, 1971, 19.
15. Kellermann, K. I. and Pauling-Toth, I. K. K. Astrophys. Letters, 8, 1971, 153.
16. Kellermann, K. I. et al. Astrophys. J., 169, 1971, 1.
17. Broten, N. W. et al. Monthly Notes Roy. Astron. Soc., 146, 1969, 313.
18. Clarke, R. W. et al. Ibid., 381.
19. Kellermann, K. I. and Pauling-Toth, I. K. K. Astrophys. J., 155, 1969, L71.
20. Schaffer, D. B., Cohen, M. H., Jauncey, D. L. and Kellermann, K. I. Astrophys. J., 173, 1972.
21. Sandage, A. R. Astrophys. J., 133, 1961, 355.
22. Sandage, A. R. Astrophys. J., 141, 1965, 1560.
23. Braude, S. Ya., Zhuk, I. N., Men', A. V. and Ryabov, B. P. Preprint No. 5, IRE AN Ukr. SSR, 1969.
24. Kellermann, K. I., Clark, B. G. et al. Astrophys. J., 161, 1970, 803.
25. Broderick, J. J. et al. Astrophys. J., 172, 1972, 299.
26. Cohen, M. H. et al. Astrophys. J., 158, 1969, L83.
27. Andrew, B. H. and Kraus, J. D. Astrophys. J., 159, 1970, L45.
28. Kraus, J. D. and Andrew, B. H. Astrophys. J., 159, 1970, L41.

/27

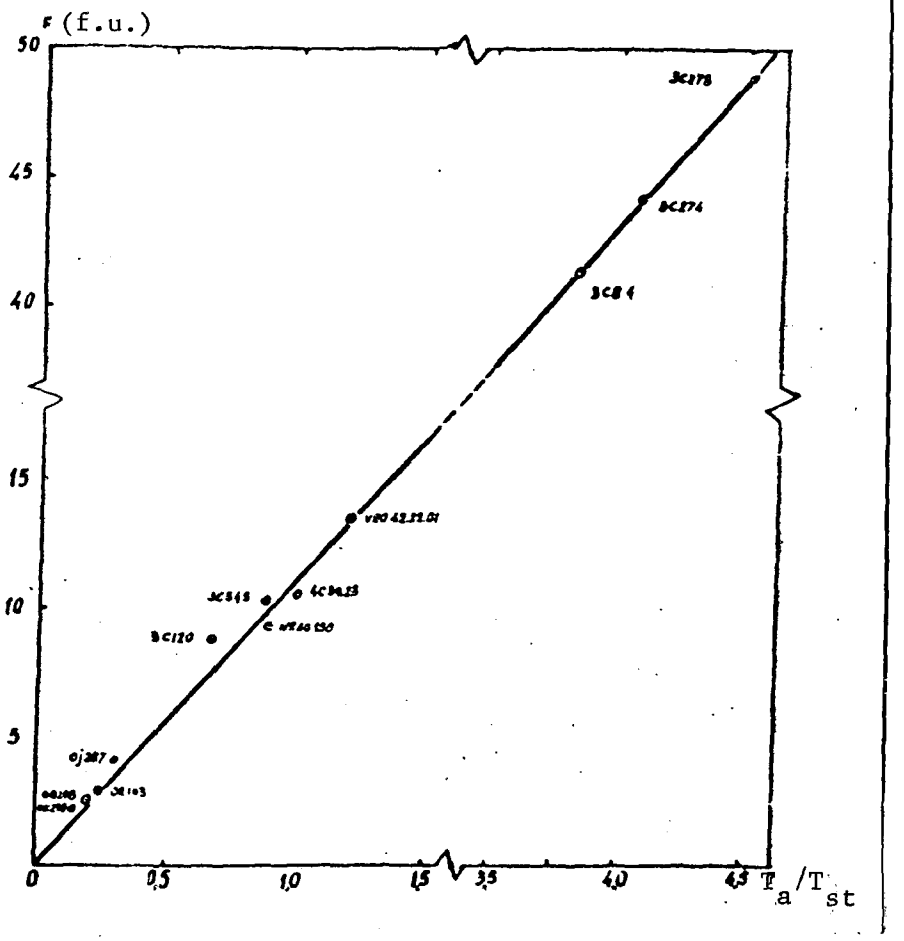

Fig. 1. Dependence of antenna temperature on the radio radiation flux density.

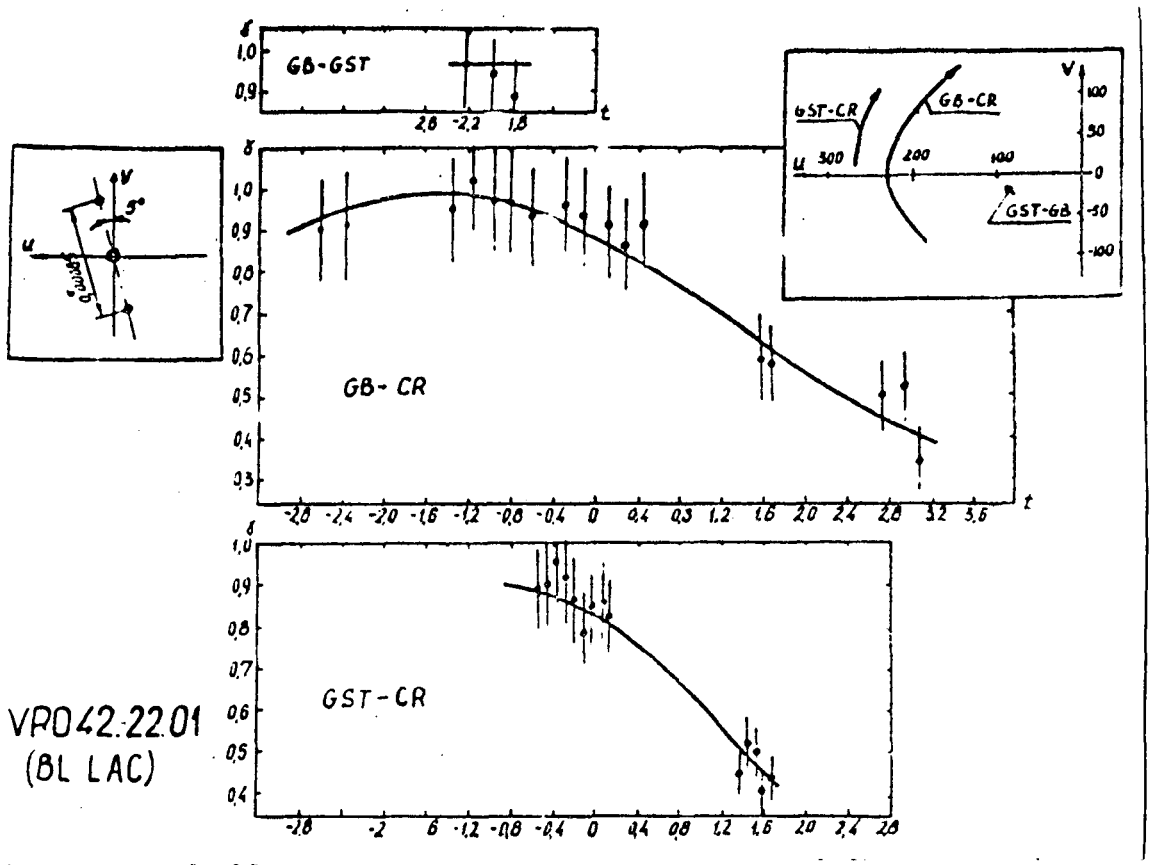

Fig. 2a

Fig. 2. Visibility function of radio sources. At the upper right: projection of the three bases on the plane of the source. The quantities u,v are plotted in millions of wavelengths.

At the left: Radio-source models giving best agreement with the experimental findings.

(a) VRO 422201
(b) NRAO 150
(c) 3C 345
(d) 4C3925
(e) 3C 84

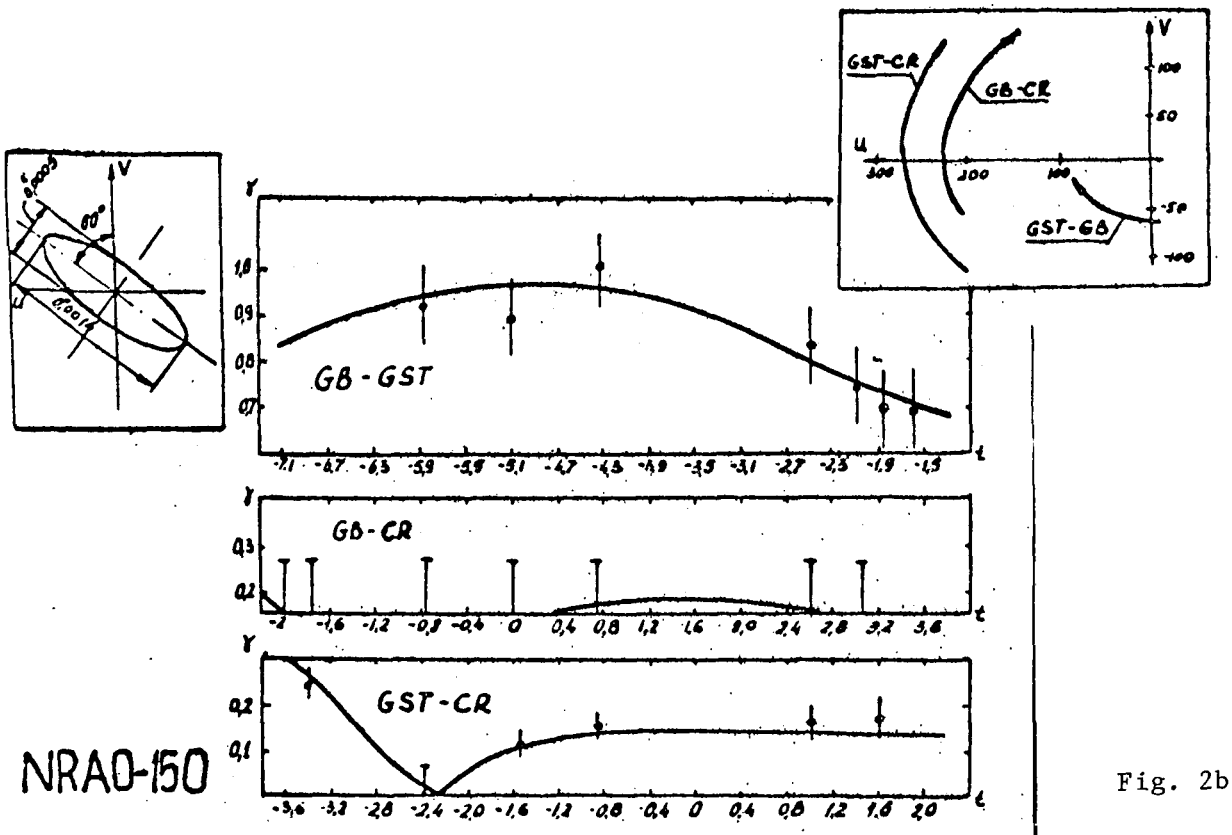

Fig. 2b

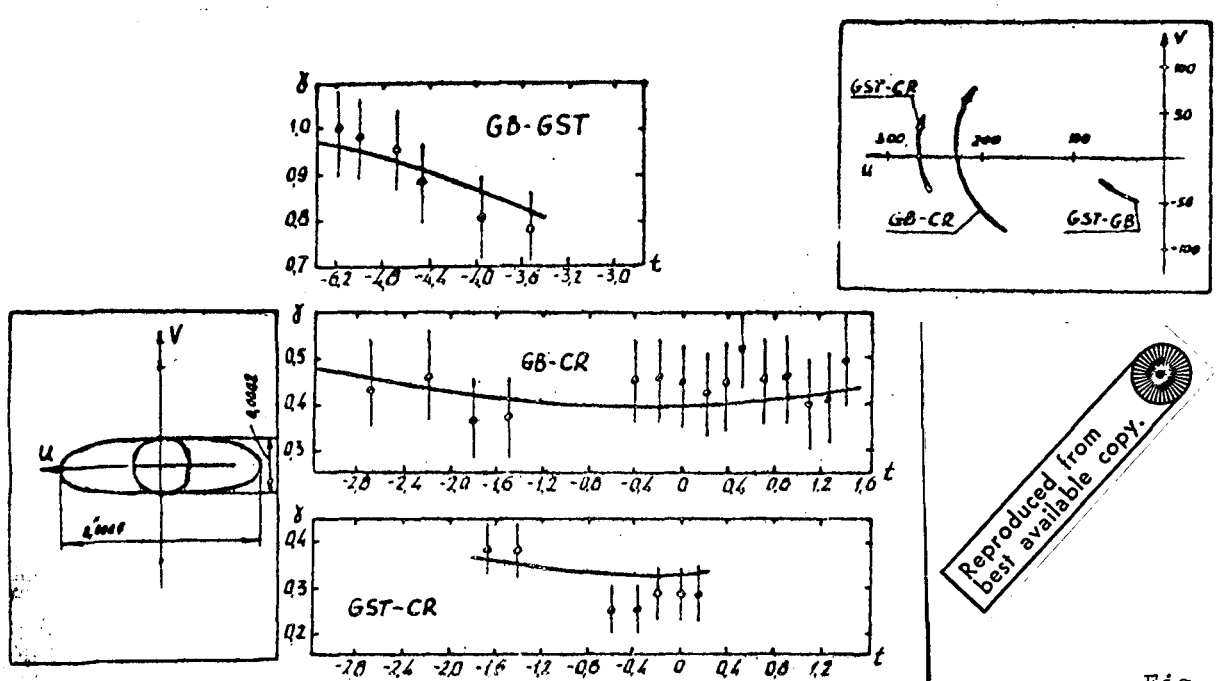

Fig. 2c

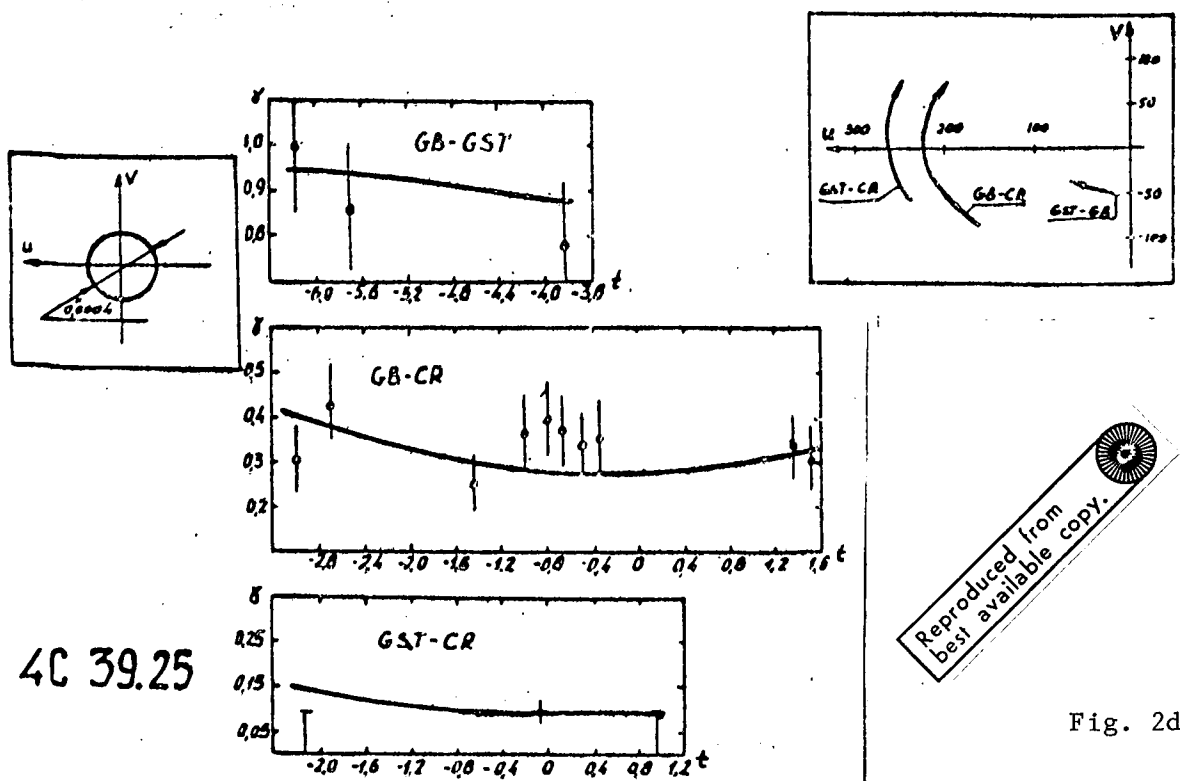

Fig. 2d

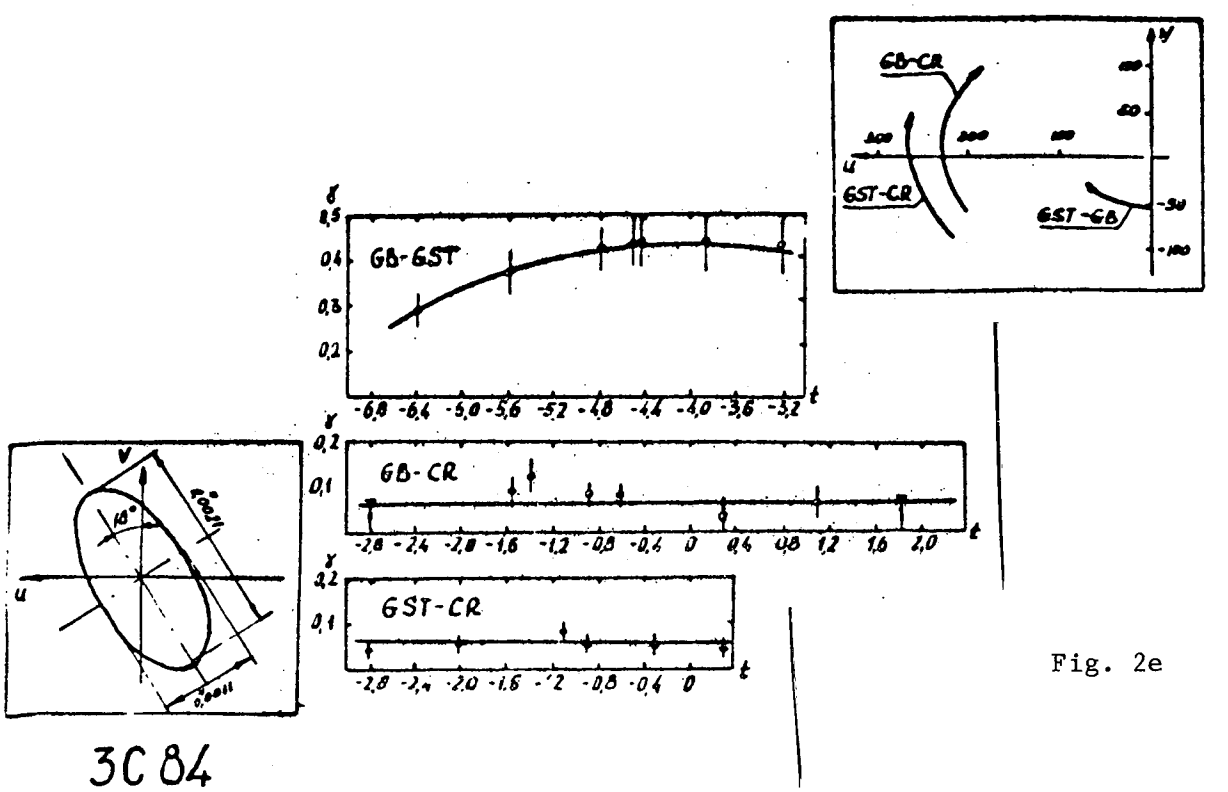

Fig. 2e

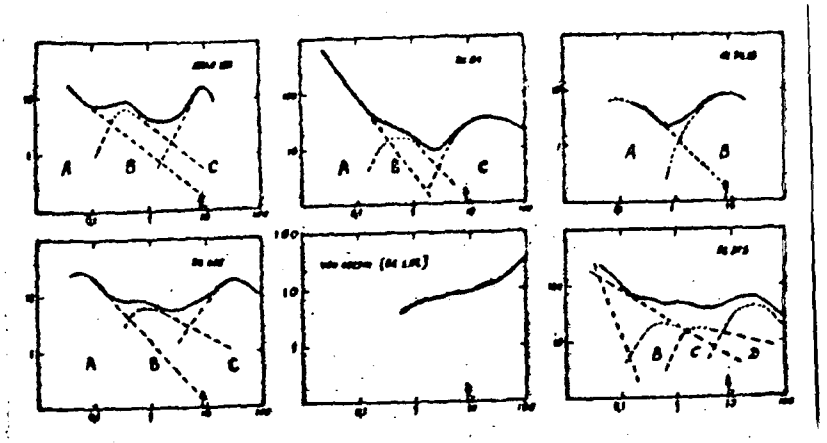

Fig. 3. Radio-source spectra. Frequency in Hz on the horizontal axis. Flux density in flux units (f.u.) on the vertical axis.

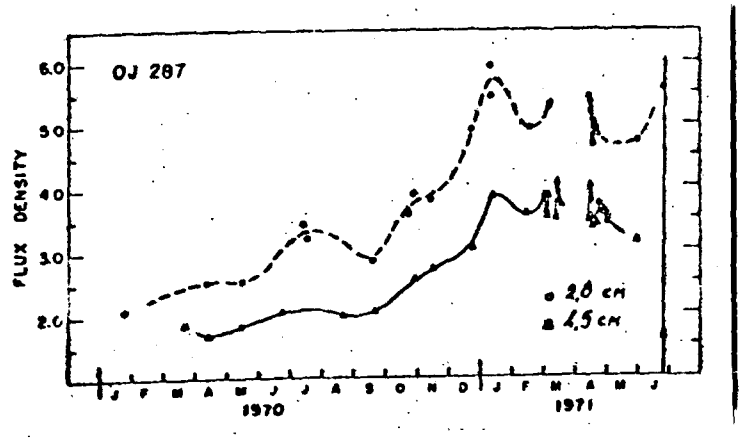

Fig. 4. Change in flux density of the source OJ 287 during 1870-1971. The arrow indicates the observing day, 25.VI.71.

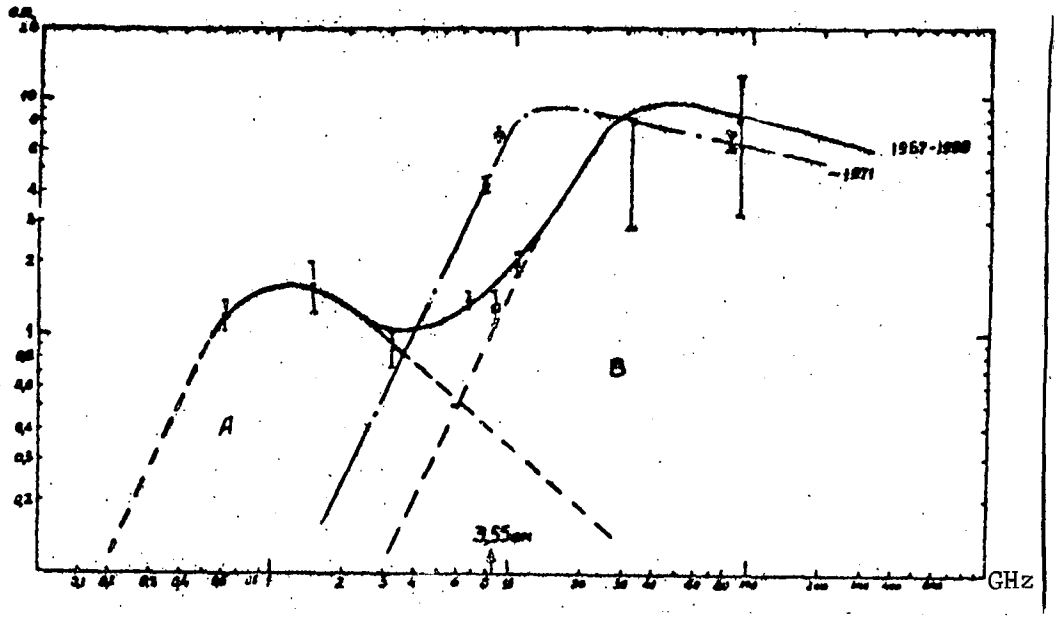

Fig. 5. Spectrum of radio-source OJ 287, constructed from the following data: x - [28]; o - [12]; □ - [11]; ✕ - [9]; ● - [5].

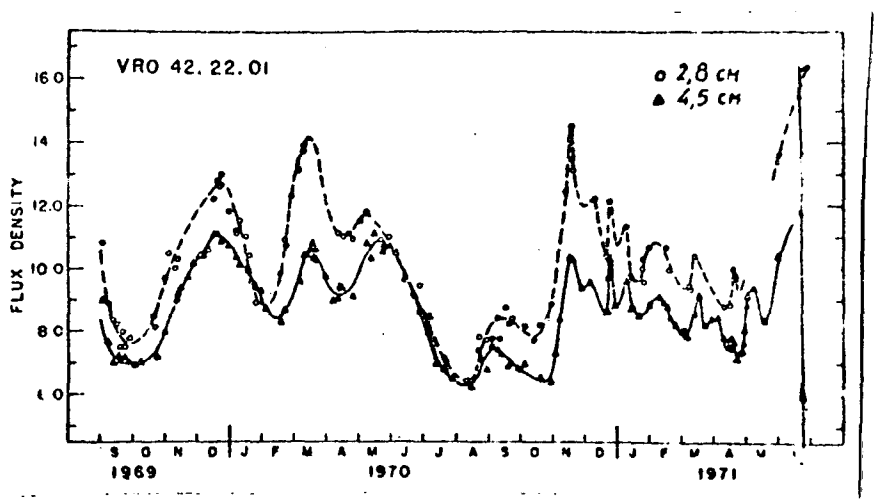

Fig. 6. Flux variation for radio source VRO 422201 during 1969-1971. The arrow marks the observing day, 25.VI.71.